Fibrillins, Fibulins, and Matrix-Associated Glycoprotein Modulate the Kinetics and Morphology of *in Vitro* Self-Assembly of a Recombinant Elastin-like Polypeptide[†]

Judith T. Cirulis,[‡] Catherine M. Bellingham,[‡] Elaine C. Davis,[§] Dirk Hubmacher,[§] Dieter P. Reinhardt,[§,#] Robert P. Mecham,[||] and Fred W. Keeley*,[‡]

Research Institute, The Hospital for Sick Children, Toronto, Canada, Department of Anatomy and Cell Biology, McGill University, Montréal, Canada, Faculty of Dentistry, McGill University, Montréal, Canada, and Department of Cell Biology and Physiology, Washington University School of Medicine, St. Louis, Missouri 63110

ABSTRACT: Elastin is the polymeric protein responsible for the properties of extensibility and elastic recoil of the extracellular matrix in a variety of tissues. Although proper assembly of the elastic matrix is crucial for its durability, the process by which this assembly takes place is not well-understood. Recent data suggest the complex interaction of tropoelastin, the monomeric form of elastin, with a number of other elastic matrix-associated proteins, including fibrillins, fibulins, and matrix-associated glycoprotein (MAGP), is important to achieve the proper architecture of the elastic matrix. At the same time, it is becoming clear that self-assembly properties intrinsic to tropoelastin itself, reflected in a temperature-induced phase separation known as coacervation, are also important in this assembly process. In this study, using a well-characterized elastin-like polypeptide that mimics the self-assembly properties of full-length tropoelastin, the process of self-assembly is deconstructed into "coacervation" and "maturation" stages that can be distinguished kinetically by different parameters. Members of the fibrillin, fibulin, and MAGP families of proteins are shown to profoundly affect both the kinetics of self-assembly and the morphology of the maturing coacervate, restricting the growth of coacervate droplets and, in some cases, causing clustering of droplets into fibrillar structures.

Elastin is an insoluble, polymeric extracellular matrix protein found in tissues requiring extensibility and elastic recoil such as large blood vessels, lung parenchyma, skin, and elastic ligaments. Elastin is synthesized from a soluble precursor called tropoelastin, which in humans has a molecular mass of approximately 70 kDa and is encoded by 34 exons. Almost all exons of tropoelastin code for either hydrophobic or cross-linking domains, with these domains generally organized in an alternating arrangement. Hydrophobic domains, often containing tandemly repeated sequences, are considered to be important for the elastomeric properties of the polymer. Cross-linking domains contain paired lysine residues usually positioned in KxxK or KxxxK spacings. These lysines are destined to take part in the formation of the covalent cross-links which stabilize the polymeric form of the protein. For a general review of elastin biochemistry, see ref *1*.

Details of the mechanism by which monomeric elastin is assembled into the polymeric extracellular elastic matrix are not yet well understood, despite the fact that organization into an appropriate architecture is likely essential for the remarkably durable mechanical properties of this matrix. A number of nonelastin matrix-associated proteins and proteoglycans have been suggested to be important for this assembly process (*2−17*). The earliest evidence for this participation was based on morphological colocalization with elastin, for example as scaffolding onto which elastin appeared to be deposited during developmental formation of the elastic matrix (*18−23*). Several groups have also demonstrated specific binding activities of these proteins and proteoglycans to tropoelastin, to each other, and to cells, in some cases identifying specific sites of binding on one or both of the participating proteins (*2−4, 6, 9−12, 14−17, 24−27*). Further evidence for the participation of these nonelastin proteins in elastic matrix assembly has come from observations of disrupted elastic matrix assembly in animals lacking expression or expressing mutant forms of these proteins (*5, 8, 13, 28, 29*) These matrix-associated proteins include members of the fibrillin, fibulin, and MAGP[1] families of proteins.

While it is clear that such extrinsic proteins have an essential role in the assembly of elastin, it is also recognized

---

* Corresponding author. Mailing address: Molecular Structure and Function Program, Research Institute, The Hospital for Sick Children, 555 University Avenue, Toronto, ON M5G1X8, Canada. Tel: (416)-813-6704. Fax: (416)-813-7480. E-mail: fwk@sickkids.ca.
[‡] Research Institute, The Hospital for Sick Children.
[§] Department of Anatomy and Cell Biology, McGill University.
[||] Department of Cell Biology and Physiology, Washington University School of Medicine.
[#] Faculty of Dentistry, McGill University.

that properties intrinsic to tropoelastin itself can contribute to the organized polymerization of elastin. For example, not only tropoelastin but also smaller polypeptides modeled on the sequences and domain structures of tropoelastin have an intrinsic ability for self-assembly into polymeric matrices (*30−35*). A characteristic of this self-assembly is the organized juxtaposition of lysine residues allowing the formation of zero-length cross-links similar to those found in the native polymer (*32, 34, 36, 37*). Moreover, polymeric materials produced by the self-assembly of elastin-like polypeptides, in the absence of any extrinsic proteins, have mechanical properties of extensibility and elastic recoil remarkably similar to those of the native elastin polymer (*34, 35*).

Fundamental to the self-assembly properties of tropoelastin and elastin-like polypeptides is their ability to undergo a temperature-induced phase separation, commonly known as coacervation. Coacervation, which occurs on elevation of the solution temperature, is indicated by the formation of a protein-rich second phase resulting in a sudden transition from a clear solution to a turbid colloidal suspension. The temperature at which this phase separation takes place is highly reproducible for a given polypeptide and has been shown to be dependent on a number of factors. These include the sequence and hydropathy of the hydrophobic domains (*33, 38*), their context in the alternating domain arrangement of tropoelastin (*38*), the number of alternating domains (*33, 38*), and the sequence and structure of the cross-linking domains (*39*). Solution conditions also affect this phase transition. Coacervation temperature decreases with increased polypeptide concentration and increased ionic strength (*33, 38*), as well as in the presence of cosolvents such as trifluoroethanol (*39*).

Coacervation in aqueous solutions is not a common property of proteins. The capacity of tropoelastin and elastin-like polypeptides to coacervate is related to their unusually hydrophobic nature, with over 80% of the amino acid residues having nonpolar character. While the ability of tropoelastin and elastin-like polypeptides to undergo coacervation has been known for many years (*30, 40−44*), the precise mechanism underlying this behavior is still not understood, although clearly it involves a shift in the hydration state of the polypeptides and may be related to a conformational transition. One of the unusual features of the coacervation process for tropoelastin and most elastin-like polypeptides is that, while the phase separation is initially reversible if the temperature of the solution is lowered below the temperature of coacervation, holding the colloid above this transition temperature for longer periods of time results in a spontaneous "maturation" process through which aligned fibrillar networks are formed that will no longer go back into solution upon lowering of the solution temperature (*30, 31, 34, 40, 41*). Eventual spontaneous formation of compacted, aligned fibrils after coacervation has been seen both for full-length tropoelastin and for smaller elastin-like polypeptides by transmission electron microscopy (*30, 34*). Similarities in appearance between such fibrillar arrays produced *in vitro* and native elastin fibers, their ability to be cross-linked via lysine side chains into polymeric matrices, and the similarity in physical properties of the polymeric materials produced by this process to those of native polymeric elastin has prompted suggestions that a coacer-

vation process may also contribute to the *in vivo* assembly of elastin polymers in the extracellular matrix (*31, 36*).

Relationships between this intrinsic capacity for self-assembly of tropoelastin and the contributions of the extrinsic nonelastin proteins to elastin polymerization and elastic matrix formation have only recently been investigated, and *in vitro* effects on coacervation of tropoelastin have recently been reported for both fibulin-5 (*12, 27*) and fibrillin-1 (*10*). Up to the present time, the only parameter that has been used to assess propensity for self-assembly of elastin-like polypeptides has been the temperature of onset of coacervation. However, onset of the phase separation represents only the first step in the eventual formation of the organized fibrillar network, and factors, including the influence of extrinsic proteins, that determine the temperature for this initial phase separation may not be the same as those governing later stages of maturation and fiber formation. Here, using a previously characterized recombinantly produced polypeptide based on the sequence and domain structure of human tropoelastin, we describe methodology for deconstructing the self-assembly of elastin-like polypeptides into stages that can be described and measured by individual parameters. Using this technique, we demonstrate that fibulins, fibrillins, and MAGP have profound and distinct effects on the kinetics of elastin self-assembly and on the morphology of the maturing elastin coacervate.

EXPERIMENTAL PROCEDURES

Expression and Purification of Elastin-like Polypeptide. Plasmid construction, recombinant expression, and purification of the elastin-like polypeptide (EP20-24-24-24-24) has been described in detail elsewhere (*38*). This polypeptide, consisting of amino acid sequences encoded by exons 20, 21, 23, 24, 21, 23, 24, 21, 23, 24, 21, 23, 24 of human elastin, has been extensively characterized, including the capacity of the polypeptide for ordered self-assembly into fibrillar, cross-linked polymers with elastin-like elastomeric properties (*34*). For each batch of EP20-24-24-24-24 produced, purity of the polypeptide was confirmed by amino acid analysis, by mass spectrometric determination of molecular weight (Advanced Protein Technology Centre, Hospital for Sick Children, Toronto, ON), and by its characteristic coacervation temperature under standard conditions (*38*). Concentration of the polypeptide was determined by amino acid analysis.

Expression and Purification of Fibulins, Fibrillins, and MAGP. Constructs for the full-length fibulin-5 and fibulin-5 deletion mutants were generously provided by Dr. Hiromi Yanagisawa, University of Texas Southwestern Medical Center, Dallas, TX. Vectors containing these constructs (*15*) were stably transfected into 293 cells, and the cells were plated in eight triple-layered flasks and selected with 100 μg/mL Neomycin G418 (Invitrogen). Once confluent, the media was changed to serum-free Dulbecco's modified Eagle medium (SF-DMEM) (Wisent Inc., Saint-Jean-Baptiste de Rouville, QC), and a total of 4 L of SF-DMEM was collected over a period of 3 weeks and stored at −20 °C. Expression and secretion of the recombinant proteins was confirmed by Western blot analysis.

For protein purification, 0.1 M PMSF was added, and the media was filtered using a 5 μm membrane (Millipore, Bedford, MA) under vacuum and then concentrated by
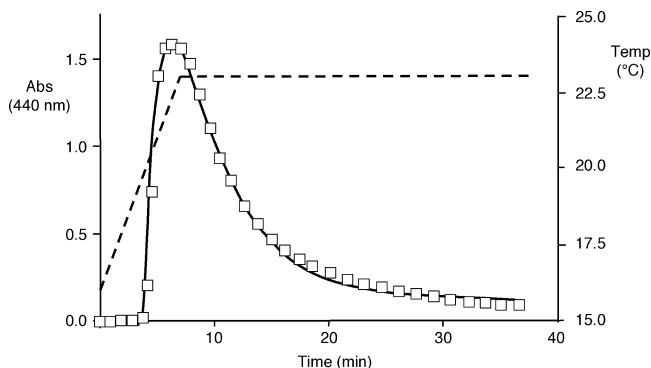
FIGURE 1: Monitoring the kinetics of coacervate formation and maturation by absorbance at 440 nm. Open squares correspond to measured absorbance. The solid line is the curve mathematically fitted to the absorption and described by the equation abs $= -a\,e^{-k_c t} + b\,e^{-k_m t} + c$ (see text). The dashed line shows the solution temperature as a function of time.
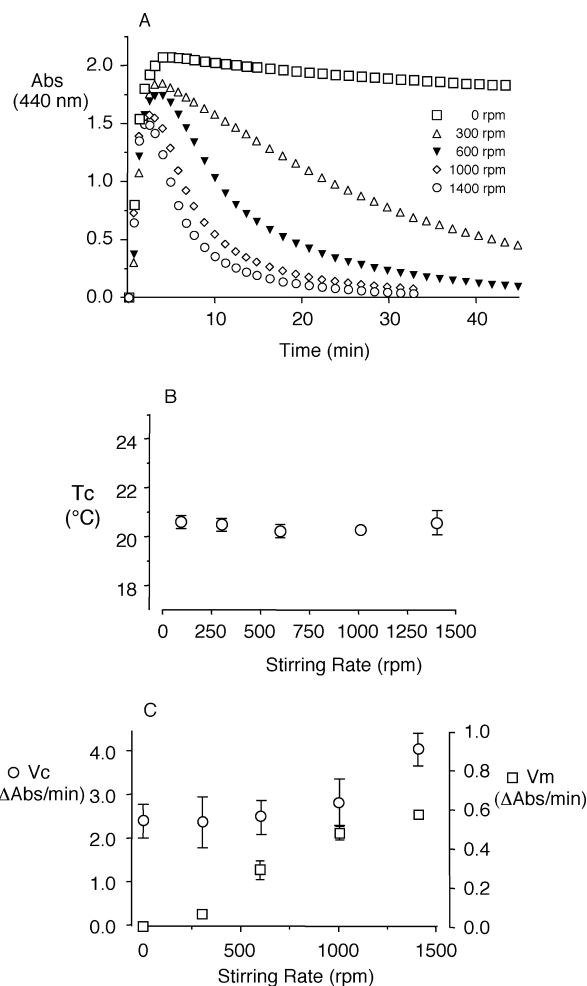

FIGURE 2: Effect of stirring rate on the kinetics of coacervate formation and maturation: (A) effect of various stirring rates on changes in absorbance with time; (B) effect of stirring rate on coacervation temperature (mean ± SD); (C) effect of stirring rate on velocity of coacervation, V_c (○), and velocity of maturation, V_m (□), parameters extracted from the equation fitted to the change in absorbance with time (mean ± SD).

ultrafiltration to ~50 mL using Amicon stirred ultrafiltration cells (series 8000 system with 10 000 MWCO, Millipore) at 4 °C. The concentrate was separated by centrifugation at 11 000g, and the supernatant was dialyzed using a Spectra/Por membrane (MWCO 12 000−14 000, Spectrum, Rancho Dominguez, CA) against filtered 500 mM NaCl in 20 mM Hepes buffer, pH 7.2, twice overnight at 4 °C. The dialyzed concentrate was passed through a 1 mL chelating HisTrap affinity column (GE Healthcare, Baie d'Urfé, QC) using an Äkta purification system (GE Healthcare). The bound protein was eluted with a linear gradient of 1 M imidazole, 500 mM NaCl, in 20 mM Hepes buffer, pH 7.2. Fractions containing the recombinant protein were pooled and dialyzed using a Spectra/Por membrane (MWCO 12 000−14 000) against 0.1 mM EDTA in Tris-buffered saline, pH 7.4, twice overnight at 4 °C. Protein concentration was determined using a BCA assay kit (Pierce, Rockford, IL).

Recombinant N- and C-terminal halves of fibrillin-1 and fibrillin-2 and recombinant fibulin-4 were produced as previously described (*16, 25*). Details of the production of recombinant MAGP-1 are described elsewhere (*2*).

Coacervation of Polypeptides. Experiments following the kinetics of coacervation were performed on a Shimadzu UV-2401PC UV−visible recording spectrophotometer (Mandel Scientific, Guelph, ON) equipped with temperature and stir rate controllers. In initial experiments (Figures 1 and 2) conditions for coacervation were as follows: the elastin-like polypeptide was dissolved at a concentration of 25 μM in coacervation buffer (50 mM Tris, pH 7.5). Prior to coacervation, the polypeptide solution was placed on ice, and NaCl was added to a final concentration of 1.5 M. The temperature of coacervation of the elastin polypeptide under these conditions is ~20 °C. Solutions for coacervation were allowed to equilibrate in a quartz cuvette for 5 min at 17 °C. The solution temperature was then increased with constant stirring at a rate of 1 °C per minute to 23 °C, a temperature at which maximum absorbance had been reached. The temperature was then held constant at 23 °C for the reminder of the experiment. Absorbance at 440 nm was automatically recorded every 18 s. Temperature of coacervation was measured as the temperature at the onset of increased absorption (*33*). Unless otherwise noted, a stirring rate of 1000 rpm was used for all coacervation experiments.

Coacervation experiments in the presence of elastic matrix-associated proteins were conducted in the same way except that the concentration of the elastin polypeptide was 6.25 μM. These proteins were added to the polypeptide solution on ice in the molar ratios indicated relative to the concentration of elastin-like polypeptide, before the addition of NaCl to 1.5 M. The coacervation temperature of the elastin polypeptide at this lower concentration is approximately 25 °C, and the maximum temperature was held at 32 °C.

Imaging Coacervation and Maturation. Images of polypeptide coacervates were obtained in real time on an Axiovert 200 epifluorescence microscope (Zeiss, Toronto, ON) with a temperature-controlled Attofluor cell chamber (Molecular Probes, Eugene, OR). The microscope was focused onto the bottom of the chamber before addition of polypeptide. The elastin polypeptide was dissolved in coacervation buffer (50 mM Tris, 1.5 M NaCl, pH 7.5) to a concentration of 100 μM. Consistent with previous observations of the relationship between concentration and coacervation temperature for similar polypeptides (*33*), the coacervation temperature of the polypeptide at this concentration was decreased to 17.5 °C. For co-coacervation experiments involving matrix-associated proteins, these proteins were added to the same

solution to a concentration of 2.0 μM. The cell chamber was filled with 1.3 mL of polypeptide solution and sealed with a glass coverslip to prevent evaporation. The cell chamber was held at a temperature of 27 °C. Coacervation was initiated immediately on the addition of the polypeptide solution to the chamber, and the initiation of coacervation was taken as time 0 for imaging. Differential interference contrast (DIC) images were obtained at various time points for 2 h. The average coacervate droplet sizes were calculated using Volocity 3.6 software (Improvision, Lexington, MA) after manually defining the edges of the droplets and sampling 60–150 droplets.

Conditions for imaging the morphology of the coacervates were not identical to those used for the spectrophotometry experiments for several reasons. In the first place, coacervation was induced by a stepwise rise in temperature to 27 °C, approximately 10 °C above the coacervation temperature of the polypeptide at the concentration used, rather than by a 1 °C/min temperature gradient in the spectrophotometry cuvette. Second, while samples were stirred in the spectrophotometry experiments, stirring was not possible in the chamber used for microscopic observations. Third, the dimensions of this chamber (18 mm in diameter, 5 mm in height) were different from those of the spectrophotometric cuvette (4 mm wide with a light path of 10 mm). Therefore, although the volumes of solution used in both experiments were approximately equal, the height of the colloidal suspension was approximately 30 mm in the cuvette compared with 5 mm in the chamber, such that any effects of settling of the coacervate droplets to the bottom of the container would be accentuated in the microscope chamber. In order to offset, at least in part, the slower maturation of the coacervate in the unstirred conditions used for microscopic observations, the polypeptide concentration was increased from 6.25 μM to 100 μM, resulting in an approximately 7-fold increase in maturation rate. This, together with longer observation times, allowed the process of maturation to be microscopically observed within a reasonable time period.

RESULTS

Modeling Kinetics of Self-Assembly. For clarity, the use of the term "coacervation" will be limited to describe only the initial phase separation event. Monitored by the spectrophotometer (Figure 1, open squares), coacervation corresponds to a rapid increase in absorption at 440 nm that begins when the coacervation temperature (T_c) is reached. Although the solution temperature is maintained constant at 23 °C, above the coacervation temperature, this initial rise in absorption is followed by a second stage, characterized by a steady decrease in absorption, eventually reaching a level of approximately 10% of the maximum absorption. This second stage is termed "maturation". The overall process is referred to as "self-assembly". Both the height of the maximum absorbance and the overall shape of the absorption curve are evidently dependent on the relative rates of the coacervation and maturation steps. In order to separate these two stages, a mathematical model (The MathWorks, Natick MA) was used to fit the entire absorbance curve:

$$\text{abs} = -a\,e^{-k_c t} + b\,e^{-k_m t} + c \qquad (1)$$

where abs is the absorbance measured at 440 nm, a and b are concentration proportionality factors, k_c is the coacervation rate constant, k_m is the maturation rate constant, and c is the final baseline absorption. This mathematical model resulted in an excellent fit to the experimental data (Figure 1, solid line). In all cases, the correlation coefficients for the double exponential fit to the corresponding experimental data were greater than 0.985, and in most cases were greater than 0.99. This double exponential fit therefore provided a means to calculate V_c, the velocity of the coacervation step (ak_c), and V_m, the velocity of the maturation step (bk_m). Together with the temperature at which coacervation is initiated, these parameters were used to quantitatively describe the kinetics of self-assembly of the elastin-like polypeptide and the modulation of self-assembly resulting from coacervation in the presence of other matrix-associated proteins.

Decreasing Absorbance during Coacervate Maturation. As shown in Figure 1, the initial rise in absorbance at 440 nm as a result of coacervation was followed by a subsequent gradual decrease during the maturation stage of self-assembly. Settling out of the coacervated material with time was clearly not an explanation for this behavior, since the sample was being stirred at a constant rate throughout the experiment (e.g., 1000 rpm in Figure 1). Moreover, the rate of fall in absorbance decreased with decreasing stirring rate and was slowest when the sample was not stirred at all (Figure 2A). Stirring rate had no measurable effect on the temperature of initiation of coacervation (T_c) (Figure 2B). Similarly, at least at stirring rates $\leq$1000 rpm, there was little or no effect on V_c, the velocity of coacervation (Figure 2C). In contrast, V_m, the velocity of maturation, was strongly dependent on stirring rate (Figure 2C), suggesting that the maturation step might be primarily a diffusion-limited process.

In order to understand what was taking place during the maturation stage of self-assembly, the morphology of the coacervate droplets were observed microscopically as a function of maturation time. Because stirring was not possible in the observation chamber, maturation would normally have taken place only very slowly (Figure 2A). This was partially offset by increasing the concentration of polypeptide from 6.25 to 100 μM. At this higher concentration, the coacervation temperature of the polypeptide is approximately 17.5 °C (Figure 3A), and maturation V_m rate is increased by approximately 7-fold. (Figure 3B,C).

Visualization of this maturation stage of self-assembly provided an explanation for the fall in absorbance with time. Droplets of coacervate 1–2 μm in diameter could be seen almost immediately after coacervation (Figure 4, left panel). With time, these droplets grew, reaching a stable size by approximately 60 min after onset of coacervation, during which time there was an increase in cross-sectional area of the droplets of more than 500-fold. Quantitation of average droplet size is shown in Figure 4, right panel. This suggested that the fall in absorption seen by spectrophotometric measurements during the "maturation" stage of self-assembly was due to coalescence of the coacervate into larger droplets with decreased ability to scatter light, consistent with the well-established inverse relationship between scattering coefficient and particle size for particulate suspensions (45).
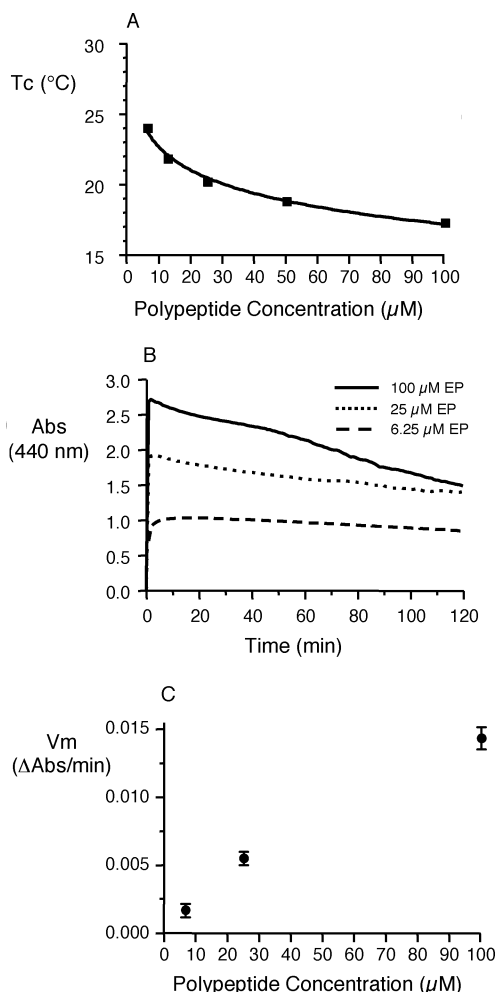
FIGURE 3: Effect of elastin polypeptide concentration on temperature of coacervation and velocity of maturation in unstirred samples: (A) Temperature of coacervation (T_c) decreases nonlinearly with increased polypeptide concentration. (B) Decrease in turbidity with time after coacervation is more rapid for higher concentrations of elastin polypeptide (EP). In all cases, the temperature was increased stepwise and held at approximately 7–10 °C above the coacervation temperature, and samples were unstirred. (C) Velocity of maturation (V_m), calculated from these tubidity vs time curves as described in Figure 1, increases with increased concentration of elastin polypeptide (mean ± SD).

Effects of Fibulins on Self-Assembly of the Elastin-like Polypeptide. Both fibulin-5 and fibulin-4 altered the kinetics of self-assembly (Figure 5). Fibulin-5, even at molar ratios as small as 1.0/0.01 (elastin polypeptide/fibulin-5), resulted in a slowing of the maturation stage (Figure 5A), and this effect was concentration dependent. Mathematical analysis of the effect of fibulin-5 on the absorption vs time relationship indicated no effect on the velocity of coacervation, V_c, but a significant effect on the velocity of maturation, V_m (Figure 5B). Fibulin-4 had a similar effect to slow maturation velocity, V_m, but this effect appeared to be less potent (Figure 5C,D). In no cases were there effects on the temperature at which coacervation was initiated, T_c (Figure 6).

Fibulin-5 mutants lacking specific regions of the protein were also investigated for their effect on coacervation kinetics of the elastin polypeptide (Figure 7). A diagramatic representation of these fibulin-5 deletion mutants is given in Figure 7A (adapted from ref *15*), and their effects on coacervation and maturation kinetics are shown in Figure 7B,C. Deletion of the first EGF domain did not alter the effect of fibulin-5

on kinetics of coacervation or maturation. However, deletion of either the elastin-binding domain or the C-terminal fibulin domain resulted in a significant attenuation of the effect of fibulin-5.

Effects of Fibrillins on Self-Assembly of the Elastin-like Polypeptide. A diagram indicating the domains contained within the N- and C-terminal halves of fibrillin-1 and fibrillin-2 (adapted from ref *25*), is shown in Figure 8. The effects of N- and C-terminal halves of fibrillin-1 and fibrillin-2 on kinetics of self-assembly are shown in Figure 9. The N-terminal half of fibrillin-1 (fibrillin-1N) clearly accelerated the rate of decrease in absorbance in a concentration-dependent manner, and this effect was apparent even at molar ratios of 1.0/0.01 (elastin polypeptide/fibrillin-1N) (Figure 9A,B). However, fibrillin-1C had no apparent effect on the kinetics of self-assembly (Figure 9A). Mathematical analysis of the coacervation curve indicated that fibrillin-1N significantly increased maturation velocity (V_m) but had no apparent effect on coacervation velocity (V_c) (Figure 9B). In contrast, neither fibrillin-2N nor fibrillin-2C had any effect on either V_c or V_m at these concentrations (Figure 9C,D). As in the case of the fibulins, none of these proteins had any detectable effect on the temperature of coacervation, T_c (Figure 6).

Effect of MAGP-1 on Self-Assembly of the Elastin-like Polypeptide. The effect of MAGP-1 on the appearance of the coacervation curves and the kinetics of coacervation and maturation of the elastin-like polypeptide is shown in Figure 10. MAGP-1 had a concentration-dependent effect to accelerate the decrease in absorbance with time. Mathematical analysis indicated a significant effect of MAGP-1 to increase maturation velocity (V_m). Although there was also an apparent increase in coacervation velocity (V_c) in the presence of MAGP-1, this difference was not statistically significant ($p = 0.054$). Again, MAGP-1 at these concentrations had no effect on the temperature of coacervation (Figure 6).

Visualization of the Effect of Fibulins, Fibrillins, and MAGP-1 on Coacervation Droplet Growth and Morphology. Microscopy was used to follow the time course of changes in the size and morphology of coacervate droplets formed in the presence of elastic matrix-associated proteins, including the N- and C-terminal halves of fibrillin-1 (Fibr-1N and Fibr-1C, respectively), fibulin-5 (Fibu-5), MAGP-1, and a combination of fibrillin-1N and fibulin-5 (Figure 11). In all cases, the concentration of the elastin polypeptide was 100 μM, and each of the matrix-associated proteins were present in molar ratios of 1.0/0.02 (elastin polypeptide/matrix-associated protein).

Five minutes after onset of coacervation, droplets were approximately 2 μm in diameter for the elastin polypeptide alone, and there was no discernible difference for the elastin polypeptide coacervated in the presence of fibrillin-1C, fibulin-5, or MAGP-1. However, in the presence of fibrillin-1N, the droplets, although similar in size, were already appearing to cluster. Furthermore, in the presence of both fibrillin-1N and fibulin-5, the droplets were clearly smaller in size and barely discernible in the focal plane of the microscope. By 30 min after coacervation, fibrillin-1N, fibulin-5, and MAGP-1 were all affecting the growth and morphology of the coacervate droplets, in contrast to fibrillin-1C, which had no effect. Fibulin-5, while clearly inhibiting the growth of the droplets, did not appear to be inducing
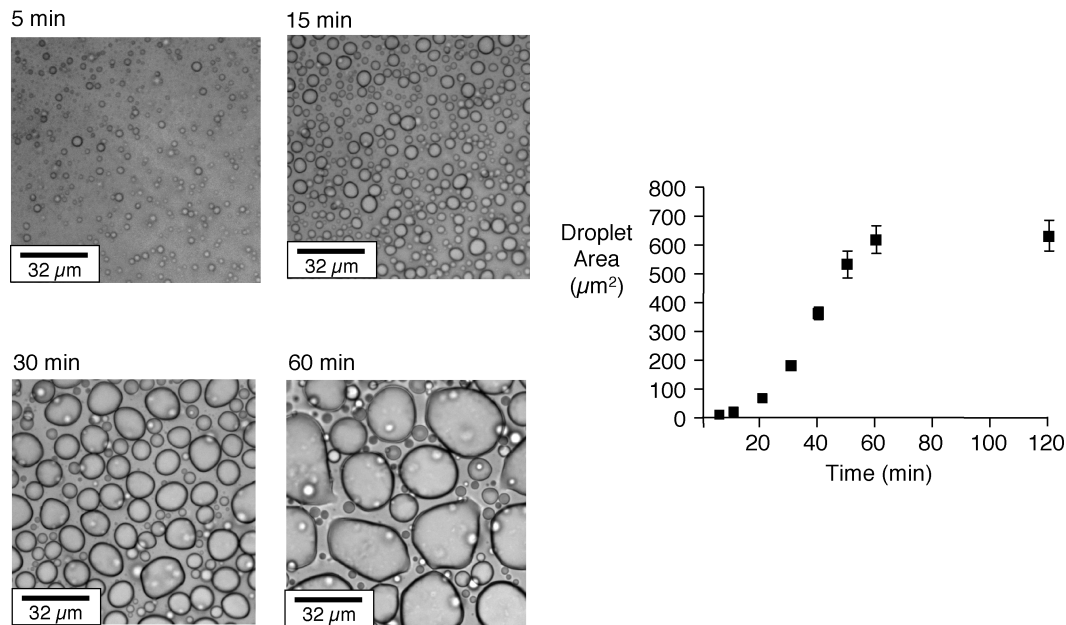
FIGURE 4: Coacervate droplet size increases with maturation time. See text for details of methodology for visualization and measurement of coacervate droplet area (mean ± SEM).
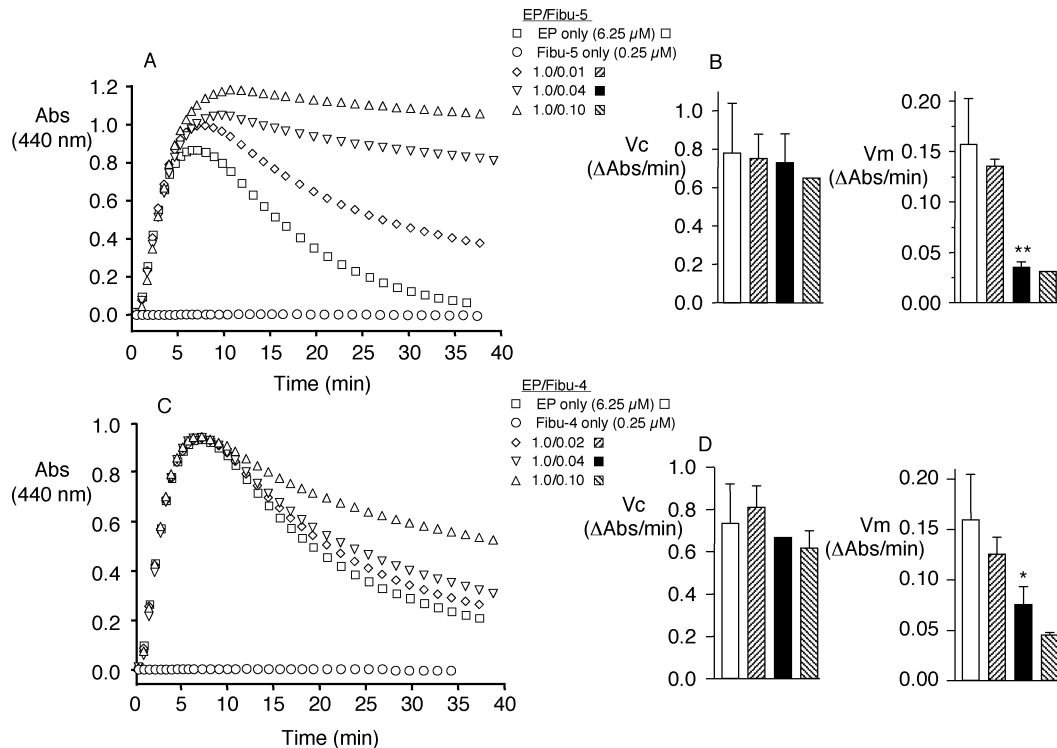

FIGURE 5: Effect of fibulin-5 and fibulin-4 on the kinetics of elastin polypeptide (EP) coacervation and maturation. Coacervation conditions and methodology for mathematical analysis of the curves are described in the text. Addition of fibulin-5 resulted in a concentration-dependent inhibition of the decrease in absorbance with time (A). Velocity of maturation was significantly reduced, while the velocity of coacervation (V_c) was not affected (B). Addition of fibulin-4 also inhibited the fall in absorbance with time in a concentration-dependent manner (C), again the result of a decreased velocity of maturation (V_m) with no change in velocity of coacervation, V_c (D). In all cases, the concentration of the elastin polypeptide was 6.25 μM. Fibulin-5 and fibulin-4 were added at the molar ratios indicated, relative to the concentration of elastin polypeptide. Mean ± SD; *, $p < 0.05$; **, $p < 0.01$ vs elastin polypeptide alone.

clustering of the droplets, as seen for MAGP-1 and especially for fibrillin-1N. In the presence of fibrillin-1N and fibulin-5 together, the droplets remained extremely small, and clustering was clearly seen at this time. These effects were even more apparent by 120 min. Higher magnification at 120 min after coacervation (Figure 12) emphasized the differences between the effects of these matrix-associated proteins and particularly demonstrated the formation of chains or "strings"

of small droplets, both with added fibrillin-1N and when fibrillin-1N and fibulin-5 were added together, creating what appeared to be a developing organized network or matrix.

DISCUSSION

While the phenomenon of coacervation either of full-length tropoelastin or elastin-like polypeptides, produced by limited
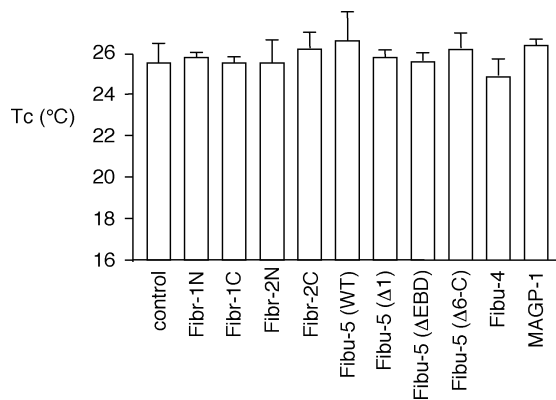
FIGURE 6: Temperature of coacervation (T_c), of the elastin polypeptide is unaffected by coacervation in the presence of matrix-associated proteins. In all cases, the concentration of the elastin polypeptide is 6.25 μM and the concentration of the matrix-associated protein is 0.25 μM (molar ratio = 1.0/0.04). Mean ± SD.

proteolysis of insoluble elastin, chemical synthesis or recombinant techniques, has been known for many years (*30, 40–44*), details of this process are still not well-understood. Similarly, while development of ordered fibrillar arrays following coacervation *in vitro* has been described using transmission electron microscopy for tropoelastin and elastin-like polypeptides (*30, 31, 34, 40, 41*), again there is little insight into the process and mechanisms through which these organized fibrils arise apparently spontaneously subsequent to coacervation. The fact that this coacervation process results in juxtaposition of lysine residues allowing zero-length cross-linking, at least in some elastin-like polypeptides (*34*), supports the view that such aggregation is not random but rather is ordered and may contribute to the organized assembly of elastic fibers *in vivo* (*31, 36*).

Previously, the only parameter available to measure propensity of tropoelastin or elastin-like polypeptides for self-assembly had been the temperature at which coacervation takes place under defined solution conditions. Here we have used a simplified, well-characterized, recombinantly produced elastin-like polypeptide containing five hydrophobic domains interspersed with four cross-linking domains (*38*) and a spectrophometric assay to deconstruct this overall process of self-assembly into "coacervation" and "maturation" stages whose velocities can be measured independently of each other and of coacervation temperature. We have previously shown that this elastin-like polypeptide not only mimics the self-assembly properties of native tropoelastin (*33, 38, 39*) but can also be cross-linked into polymeric matrixes with elastomeric properties very similar to those of the native polymer (*34*). The overall coacervation curve is the result of two processes, the relative rates of which determine the shape of the curve and the maximum turbidity measured: the rate of the coacervation process itself, causing a rise in turbidity, and the rate of the maturation of the coacervate, resulting in a decreasing turbidity. Mathematical modeling of the change in turbidity with time produced an excellent curve fit, allowing the extraction of quantitative data on velocities of the coacervation and maturation stages without making assumptions about the fundamental mechanisms of these processes. While the formation and growth of coacervate droplets have been reported elsewhere (*46–49*), this is the first instance where this process has been followed

kinetically in the presence and absence of other elastic matrix-associated proteins.

Visualization of the self-assembly process by microscopy provided information on the changes in the morphology of the coacervate droplets corresponding to the fall in turbidity during the maturation stage. Experimental conditions for the spectrophotometric and microscopic observations were necessarily different, particularly in the fact that the sample could not be stirred in the chamber for the microscopy experiments. However, the observations of an increasing droplet size over time coincident with a decreasing turbidity at a polypeptide concentration of 100 μM, without stirring, suggested that growth of coacervate droplets with time was also a plausible explanation for the decrease in turbidity seen in the spectrophotometric experiments using 6.25 μM of the polypeptide with stirring.

We have utilized this spectrophotometric assay to assess the effects of several proteins associated with elastin in elastic fibers on the various stages of this self-assembly process. These include members of the fibrillin, fibulin, and MAGP families of proteins, which are components of the microfibrillar scaffolding on which polymeric elastin is assembled *in vivo*. In recent years, with the ability for recombinant production of both full length and selected domains of these proteins, a wealth of information has emerged on their interactions, suggesting a complex, multiprotein network of associations that assist in the organized deposition of polymerized elastin in the extracellular matrix and likely control the final architecture of elastin fibers in vascular and other tissues (*2–4, 6, 9–12, 14–17, 24–27*).

Both fibulin-4 and fibulin-5 have been shown to bind to tropoelastin (*11, 14, 15, 27*), and binding of fibulin-5 to the N-terminal half of fibrillin-1 has also been reported (*11, 16*). Fibulin-5 has also been suggested to interact with cells through its N-terminal region, as part of the process of organization of the extracellular elastic matrix in the vicinity of the cell surface (*12*). In the experiments reported here, both fibulin-5 and fibulin-4, even at low molar ratios, had a marked effect to slow the maturation stage of self-assembly of the elastin-like polypeptide without significantly affecting either the coacervation temperature or the rate of coacervation. Visualization of the self-assembly process in the presence of fibulin-5 indicated that this slowing of maturation corresponded to an inhibition of the coalescence and growth in size of the coacervation droplets, resulting in a slower decrease in the measured light scattering/turbidity. The apparent decreased potency of fibulin-4 to slow maturation compared with fibulin-5 is consistent with earlier reports of stronger binding of fibulin-5 to tropoelastin compared with fibulin-4 (*14*).

Experiments with deletion mutations of wild-type fibulin-5 gave results generally consistent with those previously reported using *in vitro* solid phase binding assays and *in vivo* rescue experiments using fibulin-5 deficient mice (*12*). Deletion of the N-terminal EGF domain had no measurable effect on the ability of fibulin-5 to inhibit coacervate maturation. In contrast, deletion of the region previously identified as an elastin-binding domain (*15*) attenuated this effect substantially. Removal of the entire C-terminal portion of the fibulin-5, containing this elastin-binding domain, blocked the effect of wild-type fibulin-5 even more, although a significant activity remained even after C-terminal deletion,
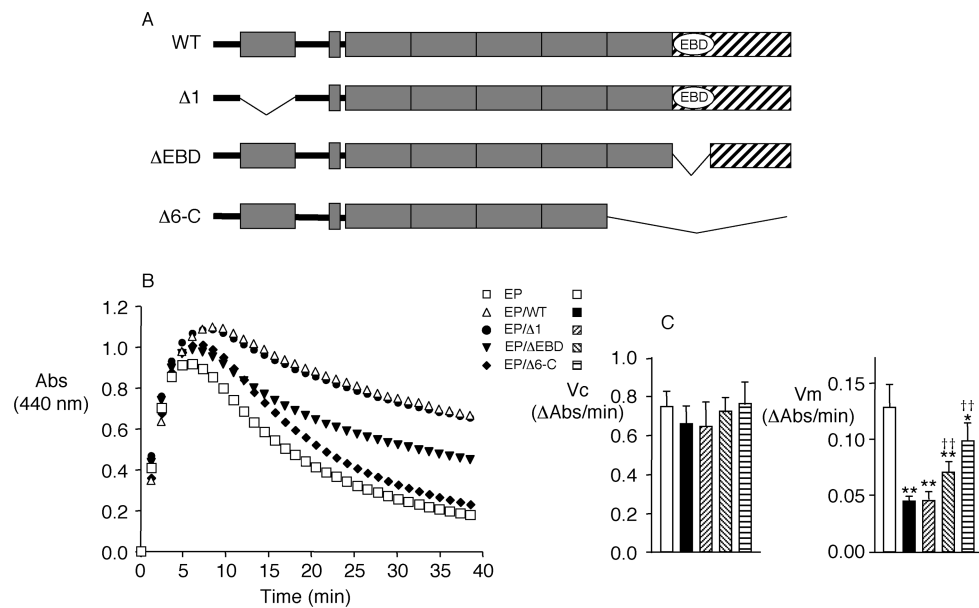
FIGURE 7: Effect of deleting regions of fibulin-5 on kinetics of coacervation and maturation of the elastin polypeptide (EP). (A) Domain structure of wild-type fibulin-5 (WT) and the fibulin-5 deletions tested (adapted from ref *15*). Shaded regions are EGF domains; hatched region is fibulin domain; EBD is elastin binding domain. (B) Effects of wild-type fibulin-5 (WT) and deletion mutations, as indicated, on change of absorption with time. (C) Effects of fibulin-5 deletions on coacervation velocity (V_c) and maturation velocity (V_m). In all cases, the concentration of elastin polypeptide was 6.25 μM and the molar ratio of elastin polypeptide/fibulin-5 was 1.0/0.04. Mean $\pm$ SD; $*$, $p < 0.05$; $**$, $p < 0.01$ vs elastin polypeptide alone; $\dagger\dagger$, $p < 0.01$ vs elastin polypeptide/WT.
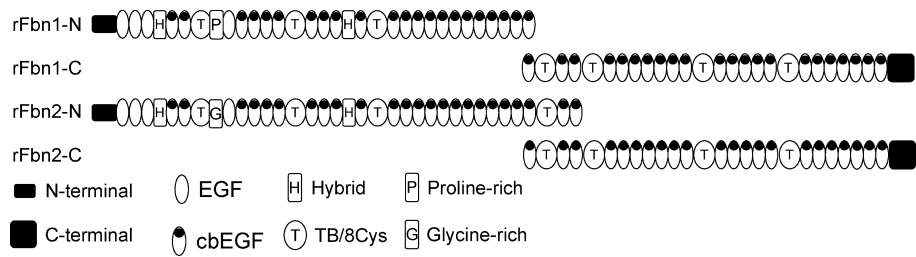

FIGURE 8: Diagram mapping domains contained in the N- and C-terminal halves of fibrillin-1 and fibrillin-2 (adapted from ref *25*).

suggesting that interactions affecting coacervate maturation may be more generally distributed on the fibulin-5 molecule.

MAGP-1 is closely associated with the microfibrillar scaffold and has been reported to bind to several other components of the extracellular matrix, including decorin and biglycan, forming a ternary complex with tropoelastin (*6*) and fibrillin-1 (*24*). MAGP-1 has also been reported to bind directly to fibrillin-1 (*4, 9*), although not to fibulin-5 (*11*), again suggesting that this protein forms a complex that influences extracellular assembly of the elastic matrix. In the experiments reported here, MAGP-1 at low molar ratios accelerated the maturation stage of self-assembly of the elastin-like polypeptide without measurably affecting the temperature at which coacervation occurred. While MAGP-1 and fibulin-5 had opposite effects on the velocity of maturation, microscopic visualization demonstrated MAGP-1 also effectively inhibited the growth of coacervate droplets. However, the additional effect of clustering of the coacervate droplets resulted in less light scattering and decreased turbidity. Note that these effects of MAGP-1 were seen despite the fact that the elastin-like polypeptide lacked the C-terminal domain of tropoelastin that has been reported to be a major binding site for MAGP-1 (*2*).

Fibrillin-1 and fibrillin-2 are also major components of the microfibrillar scaffold and have been suggested to assist in the complex architectural organization of the extracellular elastic matrix. Fibrillins have been shown to assemble into polymers through head-to-tail self-interactions (*25, 26*). Fibrillin-1 has also been demonstrated to interact with fibulin-5 (*11, 16*), and both fibrillin-1 and fibrillin-2 have been reported to bind to tropoelastin in solid phase assays but not in solution assays (*3*). Binding to tropoelastin has been mapped to the N-terminal half of fibrillin-1 (*3, 9*), and fibrillin-1 binding has also been mapped to specific regions of the tropoelastin molecule (*10*).

In the experiments reported here, the N-terminal half of fibrillin-1, again at low molar ratios, had a strong effect to accelerate the maturation stage of self-assembly of the elastin-like polypeptide, with no measurable effect on either the temperature of coacervation or the velocity of the coacervation step. As was the case for MAGP-1, the N-terminal half of fibrillin-1 strongly inhibited the growth of the droplets, but effectively decreased light scattering by causing a clustering of the droplets. A particularly striking aspect of fibrillin-1N induced clustering was the formation of "strings" of coacervate droplets rather than simple aggregates. This effect of inhibiting droplet growth and formation of clusters of small droplets was even more apparent when coacervation of the elastin-like polypeptide took place in the presence of both fibrillin-1 and fibulin-5. In contrast, neither the C-terminal half of fibrillin-1, nor the N- or C-terminal halves of fibrillin-2 had any effect on
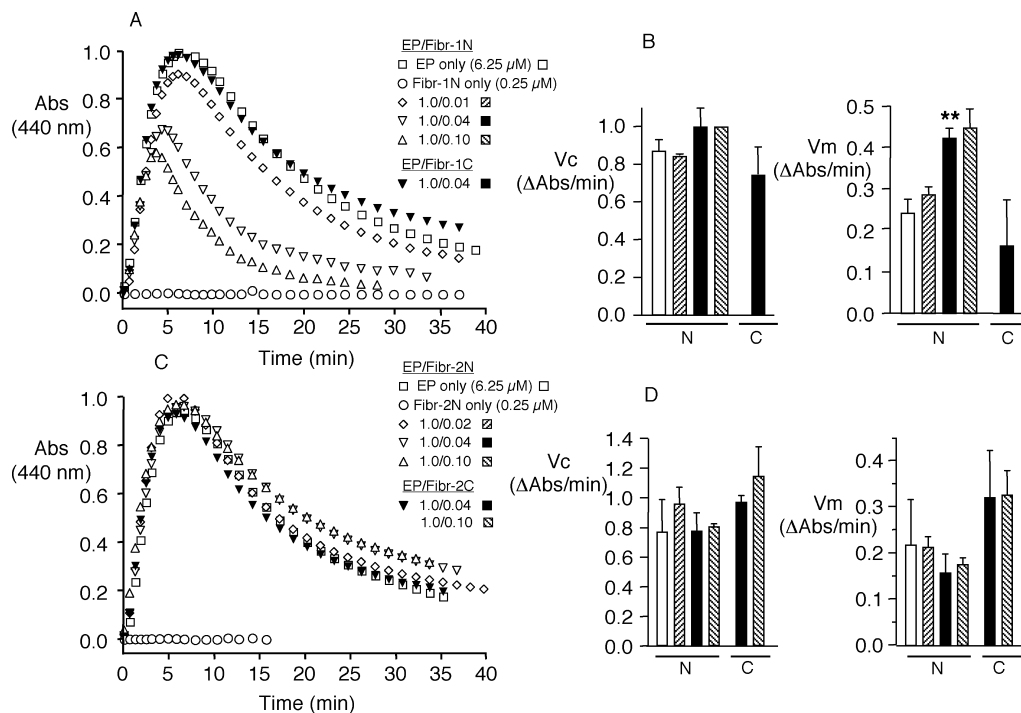
FIGURE 9: Effect of N- and C-terminal halves of fibrillin-1 and fibrillin-2 on kinetics of elastin polypeptide (EP) coacervation and maturation. Coacervation conditions and methodology for mathematical analysis of the curves are described in the text. Addition of the N-terminal half of fibrillin-1 (Fibr-1N) resulted in a concentration-dependent acceleration of the decrease in absorbance with time, while the C-terminal half of fibrillin-1 (Fibr-1C) had little or no effect (A). The effect of Fibr-1N was the result of a significant increase in the velocity of maturation (V_m), with no effect on the velocity of coacervation (V_c) (B). In contrast, neither the N-terminal or C-terminal halves of fibrillin-2 (Fibr-2N and Fibr-2C, respectively) had any significant effect on either the change in absorbance with time (C) or the magnitudes of V_c and V_m (D). In all cases, the concentration of the elastin polypeptide was 6.25 μM. Fibr-1N, Fibr-1C, Fibr-2N, and Fibr-2C were added at the molar ratios indicated, relative to the concentration of elastin polypeptide. Mean ± SD; ∗∗, $p < 0.01$ vs elastin polypeptide alone.
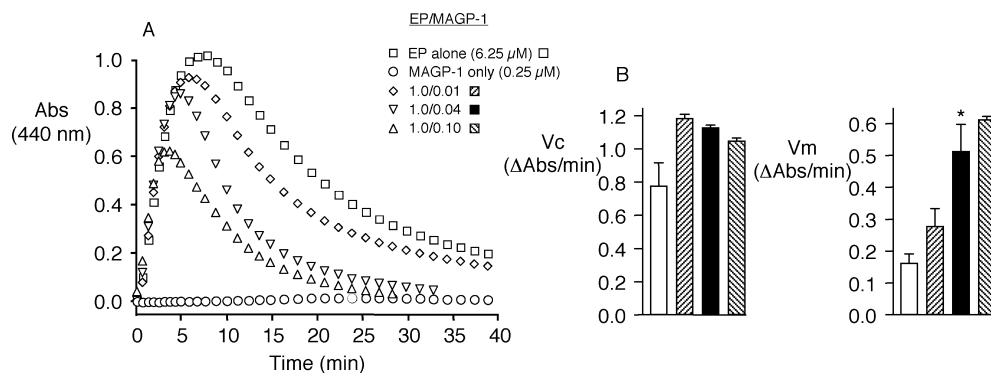

FIGURE 10: Effect of MAGP-1 on the kinetics of elastin polypeptide (EP) coacervation and maturation. Coacervation conditions and methodology for mathematical analysis of the curves are described in the text. Addition of fibulin-5 resulted in a concentration-dependent acceleration of the decrease in absorbance with time (A). Velocity of maturation (V_m) was significantly increased (B). The apparent increase in velocity of coacervation was not statistically significant ($p = 0.054$). In all cases, the concentration of the elastin polypeptide was 6.25 μM. MAGP-1 was added at the molar ratios indicated, relative to the concentration of elastin polypeptide. Mean ± SD; ∗, $p < 0.05$ vs elastin polypeptide alone.

coacervation temperature, maturation velocity, or growth of coacervation droplets. The fact that the effect of fibrillin-1 on maturation velocity was confined to the N-terminal half of this protein is consistent with previous reports that this portion of the molecule contains tropoelastin binding domains (*3, 10*). It is less clear why neither half of fibrillin-2 showed any activity although, as noted above, it had previously been reported that fibrillin-2 binding to tropoelastin appeared to be more dependent on secondary structure, and could not be measured in solid phase assays (*3*). While the elastin-like polypeptide used in these experiments, consisting of exon 20, 21, 23, and 24 sequences, does not contain sequences from exons 2−18 of tropoelastin that have

been reported to be cross-linkable to the PF2 fragment of fibrillin-1, exons 17−27 of tropoelastin, some of which are included in the elastin-like polypeptide, were also reported to bind to the PF2 fragment (*10*).

Both fibulin-5 and fibrillin-1, at molar ratios similar to those used here, have been reported to significantly lower the coacervation temperature of tropoelastin (*10, 12, 27*). In contrast, none of the matrix-associated proteins used here had any measurable effect on coacervation temperature, including those that demonstrated very strong effects on maturation of the coacervate. An explanation for this discrepancy may be related to the fact that the simplified elastin polypeptide used in these experiments included only
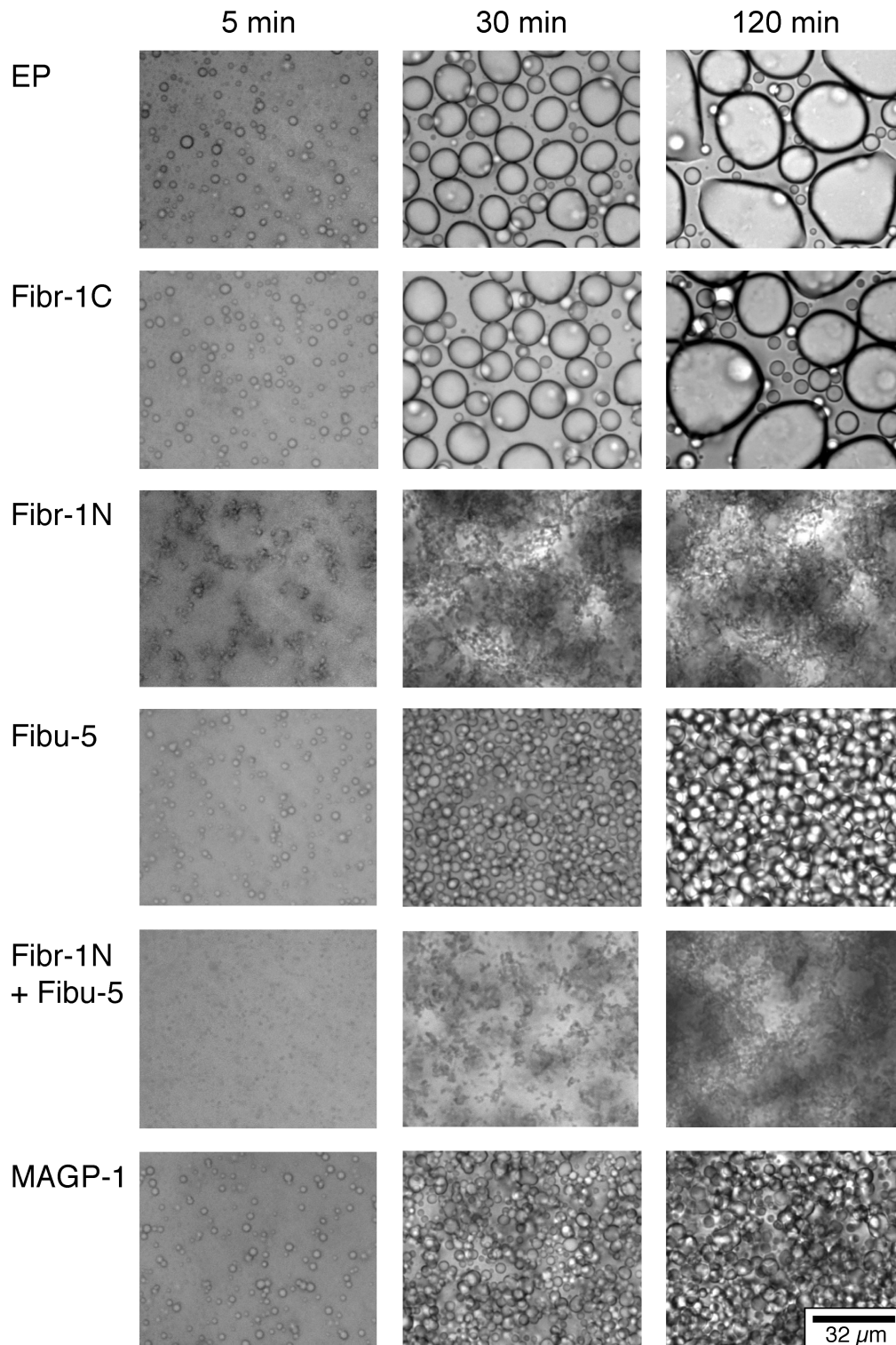
FIGURE 11: Effects of fibulin-5 (Fibu-5), N- and -C terminal halves of fibrillin-1 (Fibr-1N and Fibr-1C, respectively), MAGP-1, and a combination of Fibr-1N and Fibu-5 on growth of coacervation droplets of the elastin polypeptide (EP) with time. Images are taken at 5, 30, and 120 min after initiation of coacervation. With the exception of Fibr-1C, all of these matrix-associated proteins had the effect of inhibiting growth of the coacervation droplets. In all cases, the concentration of EP was 100 μM, and Fibu-5, Fibr-1N, Fibr-1C, and MAGP-1 were each added at a concentration of 2.0 μM (molar ratio of 1.0/0.02). In the case of Fibr-1N + Fibu-5, both proteins were present at a concentration of 2.0 μM. Scale bar refers to all panels.

a limited selection of sequences from human tropoelastin (i.e., exons 20, 21, 23, and 24), suggesting that other sequences from tropoelastin not represented in this polypeptide are specifically responsible for the reported effects on coacervation temperature.

MAGP, fibrillins, and fibulins have all been shown to be associated with the extracellular microfibrillar scaffold on which elastin assembles in the formation of elastic fibers. While elastin can still be synthesized and at least partially assembled and cross-linked in fibulin-4, fibulin-5, and fibrillin-1 knockout mice, the lack of any one of these scaffold-associated proteins results in a profound disruption in the architectural organization of the resulting elastic fibers (5, 7, 13, 29). Furthermore, mutations in fibulin-5 have
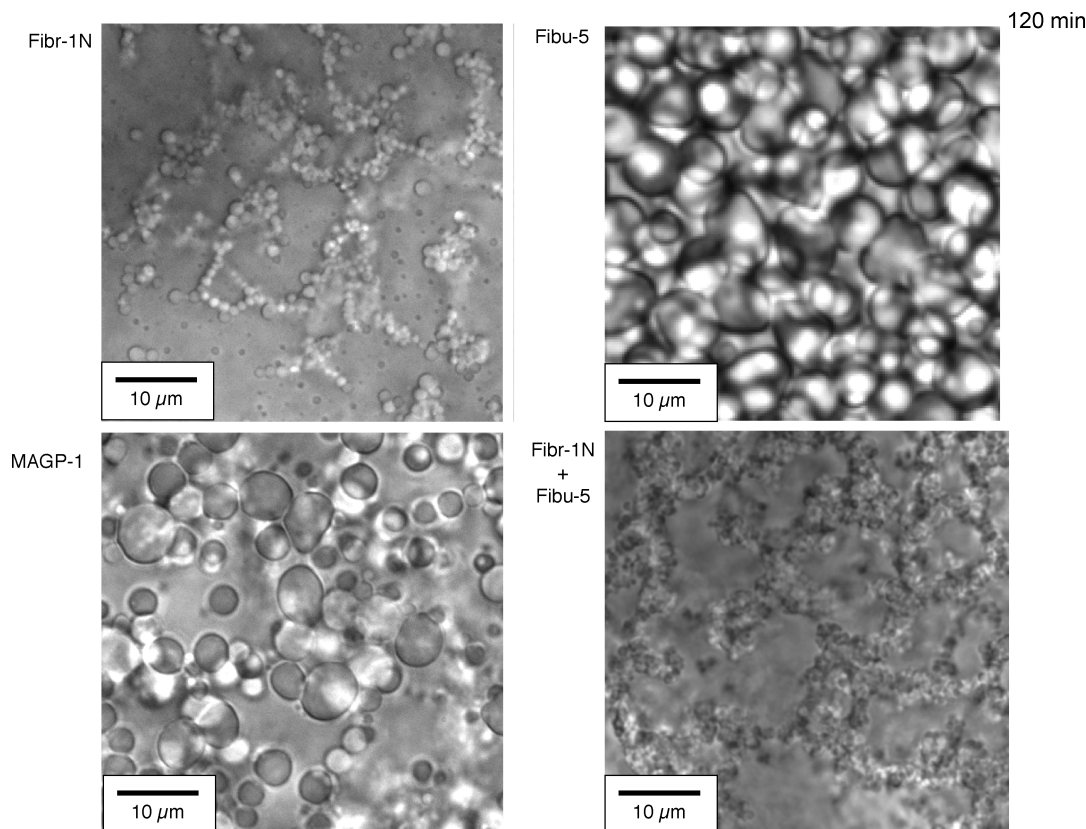
FIGURE 12: Higher magnification images of coacervation droplets 120 min after initiation of coacervation. In all cases, the concentration of the elastin polypeptide was 100 μM and Fibu-5, Fibr-1N, and MAGP-1 were each added at a concentration of 2.0 μM (molar ratio of 1.0/0.02). In the case of Fibr-1N + Fibu-5, both proteins were present at a concentration of 2.0 μM. Particularly in the case of added Fibr-1N and Fibr-1N + Fibu-5, the effect is to cluster small coacervation droplets into chains or "strings", forming an organized network.

been shown to result in recessive cutis laxa, a connective tissue disease involving disorganized elastic fibers (*28*). Particularly in situations of fibulin-4 or fibulin-5 deficiency, the secreted elastin has been reported to form abnormally large, globular shaped clumps in the extracellular matrix (*28*, manuscript submitted, E. C. Davis). Significantly, in the *in vitro* model system used here, which mimics many aspects of the self-assembly process of native tropoelastin, all of these matrix-associated proteins had the effect of strongly inhibiting growth of the coacervate droplets of elastin. The fact that these effects are seen at low molar ratios also suggests that these proteins act by stabilizing the surface of the colloidal particles and preventing them from coalescing into larger droplets.

Deposition of elastin as small droplets on the microfibrillar scaffold has been suggested to be an early stage of elastin formation, perhaps as a coacervate, which then assembles on the microfibrillar scaffold as linear arrays (*47, 48*). In the *in vitro* experiments reported here, both MAGP-1 and fibrillin-1 caused droplets to cluster, in the case of fibrillin-1 forming similar linear "strings" of coacervate droplets. Clustering of droplets of a tropoelastin coacervate on the surface of beads coated with PF2, a subfragment of the N-terminal half of fibrillin-1, has also been reported (*10*). Taken together, these observations suggest that the *in vitro* effects of these elastic matrix-associated proteins seen here may reflect an *in vivo* role to maintain a minimal size of coacervation droplet of tropoelastin and promote organized deposition of these droplets onto the microfibrillar scaffold.

This assay provides a simple and useful *in vitro* method for characterizing and quantitating the effects of matrix-associated proteins on the assembly of elastin. In contrast to solid state binding assays, which can be subject to surface artifacts, the interactions detected in this case take place in solution and with a coacervated form of elastin, more closely mimicking the *in vivo* situation. Furthermore, the assay has the advantage that it measures a functional effect of these interactions. While the use of polypeptides containing only a limited selection of the domains of human tropoelastin may prevent detection of interactions dependent on sequences not represented in this simplified elastin-like polypeptide, the fact that these domains can readily be rearranged, mutated, and replaced by other elastin sequences (*33, 38, 39*) also provides a versatile approach to isolate and map interactions with specific domains in elastin that modulate the assembly process, thus contributing to the understanding of the complex architecture of the elastic fiber that is likely responsible for the remarkable durability of its mechanical properties.

ACKNOWLEDGMENT

REFERENCES

1. Mithieux, S. M., and Weiss, A. S. (2005) Elastin. *Adv. Protein Chem. 70*, 437–461.
2. Brown-Augsburger, P., Broekelmann, T., Mecham, L., Mercer, R., Gibson, M. A., Cleary, E. G., Abrams, W. R., Rosenbloom, J, and

Mecham, R. P. (1994) Microfibril-associated glycoprotein binds to the carboxyl-terminal domain of tropoelastin and is a substrate for transglutaminase. *J. Biol. Chem. 269*, 28443–28449.

3. Trask, T. M., Trask, B. C., Ritty, T. M., Abrams, W. R., Rosenbloom, J., and Mecham, R. P. (2000) Interaction of tropoelastin with the amino-terminal domains of fibrillin-1 and fibrillin-2 suggests a role for the fibrillins in elastic fiber assembly. *J. Biol. Chem. 275*, 24400–24406.

4. Jensen, S. A., Reinhardt, D. P., Gibson, M. A., and Weiss, A. S. (2001) Protein interaction studies of MAGP-1 with tropoelastin and fibrillin-1. *J. Biol. Chem. 276*, 39661–39616.

5. Nakamura, T., Lozano, P. R., Ikeda, Y., Iwanaga, Y., Hinek, A., Minamisawa, S., Cheng, C. F., Kobuke, K., Dalton, N., Takada, Y., Tashiro, K., Ross Jr, J., Honjo, T., and Chien, K. R. (2002) Fibulin-5/DANCE is essential for elastogenesis *in vivo*. *Nature 415*, 171–175.

6. Reinboth, B., Hanssen, E., Cleary, E. G., and Gibson, M. A. (2002) Molecular interactions of biglycan and decorin with elastic fiber components: biglycan forms a ternary complex with tropoelastin and microfibril-associated glycoprotein 1. *J. Biol. Chem. 277*, 3950–3957.

7. Yanagisawa, H., Davis, E. C., Starcher, B. C., Ouchi, T., Yanagisawa, M., Richardson, J. A., and Olson, E. N. (2002) Fibulin-5 is an elastin-binding protein essential for elastic fiber development *in vivo*. *Nature 415*, 168–171.

8. Timpl, R., Sasaki, T., Kostka, G., and Chu, M. L. (2003) Fibulins: A versatile family of extracellular matrix proteins. *Nat. Rev. Mol. Cell Biol. 4*, 479–489.

9. Rock, M. J., Cain, S. A., Freeman, L. J., Morgan, A., Mellody, K., Marson, A., Shuttleworth, C. A., Weiss, A. S., and Kielty, C. M. (2004) Molecular basis of elastic fiber formation. Critical interactions and a tropoelastin-fibrillin-1 cross-link. *J. Biol. Chem. 279*, 23748–23758.

10. Clarke, A. W., Wise, S. G., Cain, S. A., Kielty, C. M., and Weiss, A. S. (2005) Coacervation is promoted by molecular interactions between the PF2 segment of fibrillin-1 and the domain 4 region of tropoelastin. *Biochemistry. 44*, 10271–10281.

11. Freeman, L. J., Lomas, A., Hodson, N., Sherratt, M. J., Mellody, K. T., Weiss, A. S., Shuttleworth, A., and Kielty, C. M. (2005) Fibulin-5 interacts with fibrillin-1 molecules and microfibrils. *Biochem. J. 388*, 1–5.

12. Hirai, M., Ohbayashi, T., Horiguchi, M., Okawa, K., Hagiwara, A., Chien, K. R., Kita, T., and Nakamura, T. (2007) Fibulin-5/DANCE has an elastogenic organizer activity that is abrogated by proteolytic cleavage *in vivo*. *J. Cell Biol. 176*, 1061–1071.

13. Carta, L., Pereira, L., Arteaga-Solis, E., Lee-Arteaga, S. Y., Lenart, B., Starcher, B., Merkel, C. A., Sukoyan, M., Kerkis, A., Hazeki, N., Keene, D. R., Sakai, L. Y., and Ramirez, F. (2006) Fibrillins 1 and 2 perform partially overlapping functions during aortic development. *J. Biol. Chem. 281*, 8016–8023.

14. Kobayashi, N., Kostka, G., Garbe, J. H., Keene, D. R., Bächinger, H. P., Hanisch, F. G., Markova, D., Tsuda, T., Timpl, R., Chu, M. L., and Sasaki, T. (2007) A comparative analysis of the fibulin protein family. Biochemical characterization, binding interactions, and tissue localization. *J. Biol. Chem. 282*, 11805–11816.

15. Zheng, Q., Davis, E. C., Richardson, J. A., Starcher, B. C., Li, T., Gerard, R. D., and Yanagisawa, H. (2007) Molecular analysis of fibulin-5 function during de novo synthesis of elastic fibers. *Mol. Cell. Biol. 27*, 1083–1095.

16. El-Hallous, E., Sasaki, T., Hubmacher, D., Getie, M., Tiedemann, K., Brinckmann, J., Bätge, B., Davis, E. C., and Reinhardt, D. P. (2007) Fibrillin-1 interactions with fibulins depend on the first hybrid domain and provide an adaptor function to tropoelastin. *J. Biol. Chem. 282*, 8935–8946.

17. Lemaire, R., Bayle, J., Mecham, R. P., and Lafyatis, R. (2007) Microfibril-associated MAGP-2 stimulates elastic fiber assembly. *J. Biol. Chem. 282*, 800–808.

18. Greenlee, T. K., Ross, R., Jr., and Hartman, J. L. (1966) The fine structure of elastic fibers. *J. Cell Biol. 30*, 59–71.

19. Toselli, P., Salcedo, L. L., Oliver, P., and Franzblau, C. (1981) Formation of elastic fibers and elastin in rabbit aortic smooth muscle cell cultures. *Connect. Tissue Res. 8*, 231–239.

20. Cleary, E. G., and Gibson, M. A. (1983) Elastin-associated microfibrils and microfibrillar proteins. *Int. Rev. Connect. Tissue Res. 10*, 97–209.

21. Mariencheck, M. C., Davis, E. C., Zhang, H., Ramirez, F., Rosenbloom, J., Gibson, M. A., Parks, W. C., and Mecham, R. P. (1995) Fibrillin-1 and fibrillin-2 show temporal and tissue-specific regulation of expression in developing elastic tissues. *Connect. Tissue Res. 31*, 87–97.

22. Brown-Augsburger, P., Broekelmann, T., Rosenbloom, J., and Mecham, R. P. (1996) Functional domains on elastin and microfibril-associated glycoprotein involved in elastic fiber assembly. *Biochem. J. 318*, 149–155.

23. Robb, B. W., Wachi, H., Schaub, T., Mecham, R. P., and Davis, E. C. (1999) Characterization of an *in vitro* model of elastic fiber assembly. *Mol. Biol. Cell 10*, 3595–3605.

24. Trask, B. C., Trask, T. M., Broekelmann, T., and Mecham, R. P. (2000) The microfibrillar proteins MAGP-1 and fibrillin-1 form a ternary complex with the chondroitin sulfate proteoglycan decorin. *Mol. Biol. Cell 11*, 1499–14507.

25. Lin, G., Tiedemann, K., Vollbrandt, T., Peters, H., Batge, B., Brinckmann, J., and Reinhardt, D. P. (2002) Homo- and heterotypic fibrillin-1 and -2 interactions constitute the basis for the assembly of microfibrils. *J. Biol. Chem. 277*, 50795–50804.

26. Marson, A., Rock, M. J., Cain, S. A., Freeman, L. J., Morgan, A., Mellody, K., Shuttleworth, C. A., Baldock, C., and Kielty, C. M. (2005) Homotypic fibrillin-1 interactions in microfibril assembly. *J. Biol. Chem. 280*, 5013–5021.

27. Wachi, H., Nonaka, R., Sato, F., Shibata-Sato, K., Ishida, M., Iketani, S., Maeda, I., Okamoto, K., Urban, Z., Onoue, S., and Seyama, Y. (2008) Characterization of the molecular interaction between tropoelastin and DANCE/fibulin-5. *J. Biochem. 143*, 633–639.

28. Hu, Q., Loeys, B. L., Coucke, P. J., De Paepe, A., Mecham, R. P., Choi, J., Davis, E. C., and Urban, Z. (2006) Fibulin-5 mutations: Mechanisms of impaired elastic fiber formation in recessive cutis laxa. *Hum. Mol. Genet. 15*, 3379–3386.

29. McLaughlin, P. J., Chen, Q., Horiguchi, M., Starcher, B. C., Stanton, J. B., Broekelmann, T. J., Marmorstein, A. D., McKay, B., Mecham, R., Nakamura, T., and Marmorstein, L. Y. (2006) Targeted disruption of fibulin-4 abolishes elastogenesis and causes perinatal lethality in mice. *Mol. Cell. Biol. 26*, 1700–1709.

30. Bressan, G. M., Castellani, I., Giro, M. G., Volpin, D., Fornieri, C., and Pasquali Ronchetti, I. (1983) Banded fibers in tropoelastin coacervates at physiological temperatures. *J. Ultrastruct. Res. 82*, 335–340.

31. Bressan, G. M., Pasquali-Ronchetti, I., Fornieri, C., Mattioli, F., Castellani, I., and Volpin, D. (1986) Relevance of aggregation properties of tropoelastin to the assembly and structure of elastic fibers. *J. Ultrastruct. Mol. Struct. Res. 94*, 209–216.

32. Bedell-Hogan, D., Trackman, P., Abrams, W., Rosenbloom, J., and Kagan, H. (1993) Oxidation, cross-linking, and insolubilization of recombinant tropoelastin by purified lysyl oxidase. *J. Biol. Chem. 268*, 10345–10350.

33. Bellingham, C. M., Woodhouse, K. A., Robson, P., Rothstein, S. J., and Keeley, F. W. (2001) Self-aggregation characteristics of recombinantly expressed human elastin polypeptides. *Biochim. Biophys. Acta 1550*, 6–19.

34. Bellingham, C. M., Lillie, M. A., Gosline, J. M., Wright, G. M., Starcher, B. C., Bailey, A. J., Woodhouse, K. A., and Keeley, F. W. (2003) Recombinant human elastin polypeptides self-assemble into biomaterials with elastin-like properties. *Biopolymers. 70*, 445–455.

35. Mithieux, S. M., Rasko, J. E., and Weiss, A. S. (2004) Synthetic elastin hydrogels derived from massive elastic assemblies of self-organized human protein monomers. *Biomaterials 25*, 4921–4927.

36. Narayanan, A. S., Page, R. C., Kuzan, F., and Cooper, C. G. (1978) Elastin cross-linking *in vitro*. Studies on factors influencing the formation of desmosines by lysyl oxidase action on tropoelastin. *Biochem. J. 173*, 857–862.

37. Mithieux, S. M., Wise, S. G., Raftery, M. J., Starcher, B., and Weiss, A. S. (2005) A model two-component system for studying the architecture of elastin assembly *in vitro*. *J. Struct. Biol. 149*, 282–289.

38. Miao, M., Bellingham, C. M., Stahl, R. J., Sitarz, E. E., Lane, C. J., and Keeley, F. W. (2003) Sequence and structure determinants for the self-aggregation of recombinant polypeptides modeled after human elastin. *J. Biol. Chem. 278*, 48553–48562.

39. Miao, M., Cirulis, J. T., Lee, S., and Keeley, F. W. (2005) Structural determinants of cross-linking and hydrophobic domains for self-assembly of elastin-like polypeptides. *Biochemistry 44*, 14367–14375.

40. Cox, B. A., Starcher, B. C., and Urry, D. W. (1973) Coacervation of alpha-elastin results in fiber formation. *Biochim. Biophys. Acta 317*, 209–213.

41. Cox, B. A., Starcher, B. C., and Urry, D. W. (1974) Coacervation of tropoelastin results in fiber formation. *J. Biol. Chem. 249*, 997–998.

42. Urry, D. W., and Long, M. M. (1977) On the conformation, coacervation and function of polymeric models of elastin. *Adv. Exp. Med. Biol. 79*, 685–714.

43. Vrhovski, B., Jensen, S., and Weiss, A. S. (1997) Coacervation characteristics of recombinant human tropoelastin. *Eur. J. Biochem. 250*, 92–98.

44. Kaibara, K., Watanabe, T., and Miyakawa, K. (2000) Characterizations of critical processes in liquid-liquid phase separation of the elastomeric protein-water system: microscopic observations and light scattering measurements. *Biopolymers. 53*, 369–379.

45. Elimelech, M., Gregory, J. Jia, X., andWilliams, R. A. (1995) Light-scattering Methods, in *Particle Deposition and Aggregation*, pp 268−272, Elsevier, New York.

46. Clarke, A. W., Arnspang, E. C., Mithieux, S. M., Korkmaz, E., Braet, F., and Weiss, A. S. (2006) Tropoelastin massively associates during coacervation to form quantized protein spheres. *Biochemistry 45*, 9989–9996.

47. Kozel, B. A., Rongish, B. J., Czirok, A., Zach, J., Little, C. D., Davis, E. C., Knutsen, R. H., Wagenseil, J. E., Levy, M. A., and Mecham, R. P. (2006) Elastic fiber formation: A dynamic view of extracellular matrix assembly using timer reporters. *J. Cell. Physiol. 207*, 87–96.

48. Czirok, A., Zach, J., Kozel, B. A., Mecham, R. P., Davis, E. C., and Rongish, B. J. (2006) Elastic fiber macro-assembly is a hierarchical, cell motion-mediated process. *J. Cell. Physiol. 207*, 97–106.

49. Osborne, J. L., Farmer, R., and Woodhouse, K. A. (2008) Self-assembled elastin-like polypeptide particles. *Acta Biomater. 4*, 49–57.